

- 1970).
- ⁵U. F. Gianola, *J. Appl. Phys.* **28**, 868 (1957).
- ⁶M. C. Wittels, *Philos. Mag.* **2**, 1445 (1957).
- ⁷N. Q. Lam and Roger Kelly, *Can. J. Phys.* **50**, 1887 (1972).
- ⁸Y. Quéré, *Ann. Phys. (N. Y.)* **5**, 105 (1970).
- ⁹G. Delsarte, J. C. Josset, J. Mory, and Y. Quéré, *Atomic Collision Phenomena in Solids*, edited by D. W. Palmer, M. W. Tompson, and P. D. Townsend (North-Holland, Amsterdam, 1970).
- ¹⁰K. L. Merkle, *Phys. Status Solidi* **18**, 173 (1966).
- ¹¹L. E. Thomas, T. Schober, and R. W. Balluffi, *Radiat. Eff.* **1**, 257 (1969); *Radiat. Eff.* **1**, 269 (1969).
- ¹²K. L. Merkle, in *Radiation Damage in Reactor Materials* (International Atomic Energy Agency, Vienna, 1969), Vol. 1, p. 159.
- ¹³K. L. Merkle, L. R. Singer, and J. R. Wrobel, *Appl. Phys. Lett.* **17**, 6 (1970).
- ¹⁴D. I. R. Norris, *Philos. Mag.* **19**, 527 (1969).
- ¹⁵A. Seeger, *Radiation Damage in Solids* (International Atomic Energy Agency, Vienna, 1962), p. 101.
- ¹⁶S. Datz, C. D. Moak, J. S. Noggle, B. R. Appleton, and H. O. Lutz, *Phys. Rev.* **179**, 315 (1969).
- ¹⁷D. S. Gemmell and J. N. Worthington, *Nucl. Instrum. Methods* **91**, 1 (1971).
- ¹⁸J. Lindhard, *K. Dan. Vidensk. Selsk. Mat.-Fys. Medd.* **34**, 1 (1965).
- ¹⁹K. Lonsdale, *Acta Cryst.* **1**, 142 (1948).
- ²⁰J. H. Barrett, *Phys. Rev. B* **3**, 1527 (1971).
- ²¹See, for example, papers presented at the International Conference on Atomic Collisions in Solids, Gausdal, 1971, in *Radiat. Eff. Vols.* **12,13** (1972).
- ²²R. Behrisch, B. M. V. Scherzer, and J. Schulze, *Radiat. Eff.* **13**, 33 (1972).
- ²³Y. Quéré, *Phys. Status Solidi* **30**, 713 (1968).
- ²⁴See, for example, H. E. Schiøtt and P. V. Thomsen, *Radiat. Eff.* **14**, 34 (1972).
- ²⁵See, for example, G. J. Dienes and G. H. Vineyard, *Radiation Effects in Solids* (Interscience, New York, 1957).
- ²⁶K. B. Winterbon, P. Sigmund, and J. B. Sanders, *K. Dan. Vidensk. Selsk. Mat.-Fys. Medd.* **37**, 1 (1970).

Energy Transfer between the Low-Lying Energy Levels of Pr^{3+} and Nd^{3+} in LaCl_3 [†]

N. Krasutsky and H. W. Moos*

Department of Physics, The Johns Hopkins University, Baltimore, Maryland 21218

(Received 29 January 1973)

The energy-transfer mechanisms acting between the low-lying energy levels of Pr^{3+} and Nd^{3+} in LaCl_3 have been investigated. In all cases studied the Pr^{3+} ions acted as donors and the Nd^{3+} ions acted as acceptors. Fluorescence-intensity measurements have been made on the $\text{Pr}^{3+} {}^3F_3$ and 3H_6 donor systems. The shape of the time decay of the $\text{Pr}^{3+} {}^3F_3$ level has been investigated. For low Pr concentrations (<2%) the excitation is transferred directly to the Nd^{3+} ions without significant migration between the Pr^{3+} ions. The experimental results are consistent with a dipole-dipole interaction mechanism with donor-acceptor energy-transfer constants of $C = 6 \times 10^{-38} \text{ cm}^6 \text{ sec}^{-1}$ for the $\text{Pr}^{3+} {}^3F_3$ donor system and $C = 2 \times 10^{-38} \text{ cm}^6 \text{ sec}^{-1}$ for the $\text{Pr}^{3+} {}^3H_6$ donor system. For Pr concentrations ≥ 2 at.% the effects of donor-donor transfer between Pr^{3+} ions are evident from both the fluorescence-intensity measurements and the shape of the decay curves; diffusion constants were obtained from these decays. The diffusion rates indicate a donor-donor transfer constant of $C \approx 3 \times 10^{-38} \text{ cm}^6 \text{ sec}^{-1}$ for Pr^{3+} ions excited to the 3F_3 manifold. Diffusion-limited decay was observed but the limit of fast diffusion was not reached.

I. INTRODUCTION

The transfer of visible and near-infrared electronic excitation between spatially separated ions in solids has been a topic of interest for several years. The effects of transfer from a donor ion to an acceptor ion of a different species have been studied and, in addition, several experiments have been performed which demonstrated the effects of rapid donor-donor transfer, which allows the excitation to migrate to the vicinity of an energy acceptor. Only recently have the combined effects of both donor-donor transfer and donor-acceptor transfer been studied quantitatively in the same system. Weber¹ has shown clearly the effects of donor-donor transfer in Cr^{3+} -doped $\text{Eu}(\text{PO}_3)_3$

glass. He was able to vary the donor-donor transfer rate by changing the temperature of the sample and hence the relative population of the Stark components in the donor excited-state manifold. A similar study was made by Van der Ziel *et al.*² in $(\text{Y}_{1-x}\text{Tb}_x)_3\text{Al}_2\text{O}_7$. In this case impurity ions acted as acceptors. Watts and Richter³ have studied the transfer from Yb^{3+} to Ho^{3+} ions in YF_3 . They were able to vary both donor and acceptor concentrations but the acceptor concentrations were rather high owing to the nonresonant nature of the donor-acceptor transfer.

The present study was undertaken to determine the parameters governing resonant energy transfer in a system in which both donor- and acceptor-ion concentrations were known and could be varied

independently. The low-lying energy levels of Pr^{3+} and Nd^{3+} in LaCl_3 were chosen for this study because of the existence of several energy matches between the energy levels of these ions. For all energy-transfer schemes studied Pr^{3+} acted as the donor and Nd^{3+} as the acceptor. It was possible to study the direct donor-acceptor transfer and the donor-donor transfer by varying the dopant concentrations.⁴

II. EXPERIMENTAL TECHNIQUES

A. Crystal Growth and Mounting

The samples used for these experiments were all polycrystalline masses of LaCl_3 with varying amounts of praseodymium and neodymium dopants. The samples were all grown and mounted in an identical manner and the fluorescent intensities of the samples were measured relative to each other.

The polycrystalline samples were formed when the molten chloride was allowed to cool rapidly. This reduced the possibility of any preferential zone crystallization between dopant and host ions.

B. Experimental Apparatus

The pump light used for all of the experiments was a 625-W tungsten-iodine lamp. A 25-m $f/3.6$ monochromator and semiconductor filters were used to isolate the desired wavelength in the pump beam. All the measurements were made at 4.2 °K.

For the intensity measurements the fluorescence light coming off at right angles to the pump beam was focused onto the entrance slit of a 0.3-m $f/5.3$ monochromator by a spherical mirror. A PAR model-BZ-1 mechanical chopper and any necessary order filters were placed in this path. An off-axis ellipsoidal mirror was used to focus the light from the exit slit of the fluorescence monochromator onto an InAs photovoltaic detector. The signal from the detector was amplified and sent to a PAR HR-8 lock-in amplifier.

The time decay of the ${}^3F_3 \rightarrow {}^3H_6$ Pr^{3+} fluorescence was measured using a continuously variable vacuum-mounted mechanical chopper with a two-bladed wheel in the pump beam. A 2-mm slit was placed in front of the chopper blade and the pump-light cutoff time was determined by the time which it took the chopper blade to cross the slit. An interference filter with a peak at 1.62 μm and a bandwidth of 0.37 μm was used to isolate the ${}^3F_3 \rightarrow {}^3H_6$ Pr^{3+} transition. The light which passed through this filter was then focused onto the InAs detector. The output of the detector was amplified and sent to a Fabri-tek model-952 high-speed digitizer; each scan was then stored and averaged by a Fabri-tek model-1062 instrument computer.

Each sweep of the digitizer was initiated slightly before the chopper blade crossed the pump-light path so that the entire decay could be followed.

III. THEORETICAL BACKGROUND

A mechanism for direct transfer of electric excitation between spatially separated ions via the overlap of their near-zone electric dipole fields was first proposed by Förster.⁵ Förster's work was extended by Dexter⁶ to include multipolar coupling and by Inokuti and Hirayama⁷ for exchange coupling.

The form of the energy-transfer interaction can be used to determine the time decay and intensity of the donor fluorescence under different types of excitation.

Consider first the case of a random distribution of acceptor ions and no interaction between donor ions. If the donor-acceptor interactions are due to electric multipolar coupling the transfer rate can be written as an inverse power of R , the donor-acceptor separation, $W(R) = CR^{-s}$, where C is a constant independent of R . The time decay of the donor fluorescence following flash excitation is then given by⁷

$$\phi(t) = \phi(0) \exp\left[-t/\tau_0 - \frac{4}{3} \pi \Gamma(1 - 3/s) \times N_a R_0^3 (t/\tau_0)^{3/s}\right], \quad (1)$$

where $s = 6, 8,$ and 10 , respectively, for the dipole-dipole, dipole-quadrupole, and quadrupole-quadrupole interactions. N_a is the acceptor concentration and R_0 is the "critical transfer distance." It is that separation between donor and acceptor pairs at which the probability for energy transfer between them is equal to the intrinsic donor decay probability. τ_0^{-1} is the intrinsic decay rate of the donor ion due to radiative decay and phonon emission.

In the case where the pump light is allowed to strike the sample for a time long enough for steady-state conditions to be established and is then cut off sharply, the relative donor fluorescence intensity at any time t after cutoff is given by

$$\phi_s(t) = \frac{\int_t^\infty \phi(t') dt'}{\int_0^\infty \phi(t') dt'}. \quad (2)$$

The ratio of the intensity of the fluorescence seen from a sample which contains acceptor ions to the intensity from an identical sample in the absence of acceptors, is the donor luminescence yield η/η_0 :

$$\eta/\eta_0 = I/I_0 = \tau_0^{-1} \int_0^\infty \phi(t) dt. \quad (3)$$

If donor-donor transfer is present $\phi(t)$ and hence $\phi_s(t)$ will be altered; however, relationships (2) and (3) remain valid. In this case the decay

of the donor population is given by a solution of

$$\frac{\partial \phi(r, t)}{\partial t} = \frac{1}{\tau_0} \phi(r, t) - D \nabla^2 \Psi(r, t) + \sum_i V(|r - r_i|) \Psi(r, t). \quad (4)$$

D is the diffusion constant and is determined by the donor-donor transfer rate. $V(r)$ is the donor-acceptor transfer rate. The equation has been solved numerically for the case of dipole-dipole coupling between the ions.

In the case of the dipole-dipole interaction the asymptotic behavior of $\phi(t)$ has been determined.⁸ Using the scattering-length method, it is exponential with the decay rate,

$$1/\tau = 1/\tau_0 + 4\pi DN_a \rho; \quad (5)$$

ρ is a length defined by

$$\rho = 0.68(C/D)^{1/4}. \quad (6)$$

Yokota and Tamimoto⁹ have obtained a more general solution of Eq. (4) using the method of Padé approximants:

$$\phi(t) = \phi(0) \exp \left[\frac{t}{\tau_0} - \frac{4}{3} \pi^{3/2} N_a (Ct)^{1/2} \times \left(\frac{1 + 10.87z + 15.5z^2}{1 + 8.743z} \right)^{3/4} \right]. \quad (7)$$

This formula is identical to Eq. (1) for small t and approaches a value similar to Eq. (5) for large t , the difference being due to the low order of the Padé approximate used in Eq. (7).²

IV. $\text{LaCl}_3:\text{Pr}^{3+}, \text{Nd}^{3+}$

In all the cases studied here the Pr^{3+} ions acted as donors and the Nd^{3+} ions as the acceptors. The range of Pr concentration used was from 0.025 to 20 at. % and the Nd concentration from 0.002 to 5 at. %.

The low-lying energy levels¹⁰ (Fig. 1) of Pr^{3+} and Nd^{3+} were chosen for this study because of the existence of several resonant energy matches. For Pr^{3+} ions excited into the 3F_3 level the resonant transfer mechanism with Nd^{3+} ions still active at 4.2 °K are shown in Figs. 2(a)–2(c). For Pr^{3+} ions excited into the 3H_6 level the resonant transfers with Nd^{3+} ions at 4.2 °K are shown in Figs. 2(d) and 2(e). At elevated temperatures there exist possible resonant-energy-transfer matches within the Pr^{3+} energy-level system alone, by which the Pr^{3+} ions in the 3F_3 and 3H_6 can be deexcited. These transfers have been studied previously¹¹ and if active would only serve to complicate the transfers under study. For this reason all experiments were performed at 4.2 °K.

Experimentally the 3F_3 Pr^{3+} energy level was

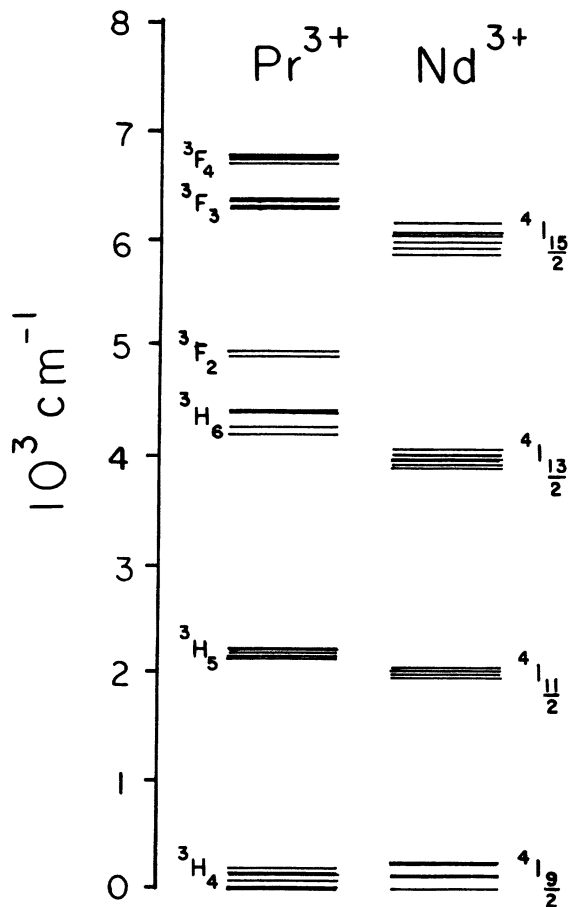


FIG. 1. Low-lying energy levels of Pr^{3+} and Nd^{3+} in LaCl_3 .

populated by using pump light which coincided with the ${}^3H_6 \rightarrow {}^3F_4$ Pr^{3+} transition. The ions excited into the 3F_4 level relax rapidly ($< 1 \mu\text{sec}$)¹² into the 3F_3 level. Similarly the 3H_6 level was populated by pumping the ${}^3H_4 \rightarrow {}^3F_2$ transition. By using transitions which were well separated from any Nd^{3+} transition it was possible to avoid pumping any Nd^{3+} ions directly and so the Nd fluorescence seen could be attributed to energy transfer from the Pr^{3+} ions.

V. RESULTS

A. ${}^3F_3 \rightarrow {}^3H_4$ Intensity Measurements

The intensity of the ${}^3F_3 \rightarrow {}^3H_4$ fluorescence under continuous excitation of the ${}^3H_4 \rightarrow {}^3F_4$ transition was measured for various Pr- and Nd-dopant concentrations in LaCl_3 . Three typical spectra are shown in Fig. 3. They are for $\text{LaCl}_3:0.25\text{-at.}\% \text{ Pr}$ [Fig. 3(a)], for $\text{LaCl}_3:0.25\text{-at.}\% \text{ Pr}, 0.1\text{-at.}\% \text{ Nd}$ [Fig. 3(b)], and $\text{LaCl}_3:0.25\text{-at.}\% \text{ Pr}, 0.5\text{-at.}\% \text{ Nd}$ [Fig. 3(c)]. The line shapes are slit limited and the individual components of the ${}^3F_3 \rightarrow {}^3H_4$ transition

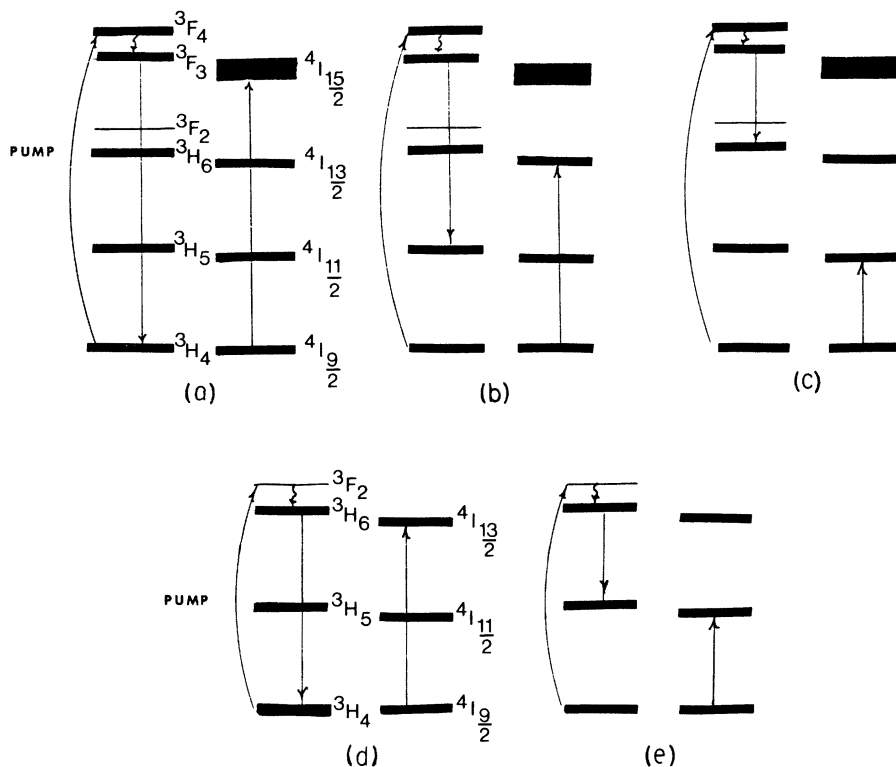


FIG. 2. Energy-transfer schemes for 3F_3 and 3H_6 donor systems.

are not resolved. The line at $1.7 \mu\text{m}$ corresponds to the transition from the ${}^4I_{15/2}$ manifold of Nd^{3+} to the lowest level of the ${}^4I_{9/2}$ manifold of Nd^{3+} . [The 0.5-at.% Nd sample, Fig. 3(c), is optically thick to this radiation and so there is a change in the ratio of the intensity seen from the different components of the ${}^4I_{15/2} \rightarrow {}^4I_{9/2}$ transition in going from Fig. 3(b) to 3(c).]

The intensity of the ${}^3F_3 \rightarrow {}^3H_4$ transition was measured for a wide range of concentrations of Pr and Nd in LaCl_3 . Radiative reabsorption was not a problem because the transition to the lowest level of the ground state was very weak. In Fig. 4, the fluorescent intensities are normalized so that when the energy transfer to Nd is negligible (≤ 0.001 -at.% Nd) the intensity is set equal to 1. This plot then displays η/η_0 for donor energy transfer. The concentrations shown in this plot are the nominal values based on the starting oxide mixtures used in growing the samples. Most of the departures of the plots from a smooth set of curves is attributable to departures of the final crystal-dopant concentrations from the original oxide concentrations. There does not appear to be any macroscopic variation in concentration within the final samples themselves.

The η/η_0 curves for the 0.025-, 0.1-, and 0.25-at.% Pr, samples (Fig. 4) are not distinguishable from each other within experimental error. If donor-donor transfer between Pr ions were im-

portant at these concentrations we would expect a large change in the shape of the η/η_0 curves after a factor of 10 change in donor concentration. The η/η_0 curves for the samples containing $\geq 2\%$ Pr do fall below the curves for the lower concentrations, indicating that donor-donor transfer is aiding in the decay of the 3F_3 level. This conclusion is borne out by time-resolved measurements of the decay of the 3F_3 level (Sec. VB).

The solid line shown in Fig. 4 is η/η_0 for the dipole-dipole interaction. This curve is plotted using a value for C of $C = 6 \times 10^{-38} \text{ cm}^6 \text{ sec}^{-1}$. This corresponds to a "critical transfer distance" of $R_0 = 17 \text{ \AA}$.

An attempt was made to use the relative fluorescence intensities seen from the Pr^{3+} and Nd^{3+} ions in the $1.5 \rightarrow 3.0\text{-}\mu\text{m}$ region to determine the dominant transfer scheme. Unfortunately the fluorescence from the $\text{Nd}^{3+} {}^4I_{15/2} \rightarrow {}^4I_{9/2}$ and ${}^4I_{13/2} \rightarrow {}^4I_{9/2}$ transitions was strongly reabsorbed by the samples even at Nd concentrations as low as 0.1%. In addition water vapor and CO_2 absorption were a problem in the region beyond $2.5 \mu\text{m}$. These problems coupled with the fact that some of the possible transitions lie beyond the detector range precluded a complete determination of where all of the energy originally in the $\text{Pr} {}^3F_3$ level went. However, a sufficient number of transitions could be observed to distinguish be-

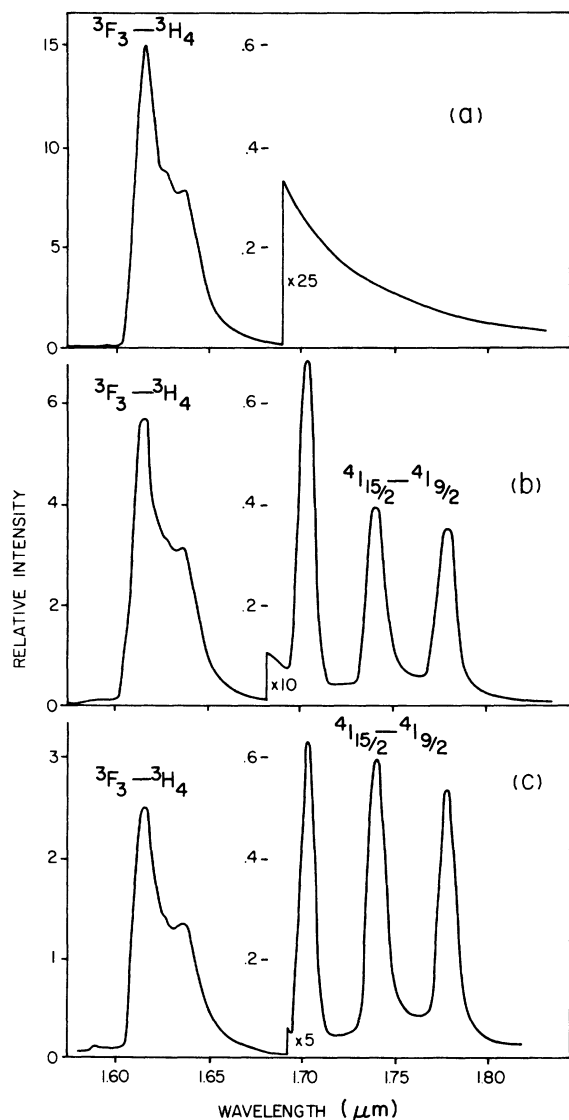


FIG. 3. Intensity trace pumping ${}^3F_3 \rightarrow {}^3H_4$ transition. (a) LaCl_3 : 2-at. % Pr, (b) LaCl_3 : 2-at. % Pr, 0.05-at. % Nd, (c) LaCl_3 : 2-at. % Pr, 0.05-at. % Nd.

tween the effects of each of the proposed energy-transfer schemes. At low concentrations ($\leq 2\%$), the transfer shown in Fig. 2(a) appears to dominate, while for the higher concentrations a strong line from the ${}^4I_{13/2} \rightarrow {}^4I_{9/2}$ transition is observed indicating the transfer process shown in Fig. 2(b) is also a strong contribution to the deexcitation of the ${}^3F_3 \text{Pr}^{3+}$ donor ions. This change in the relative effectiveness of the three transfer processes may have been due to shifts in the position of the energy levels with increasing Pr concentration. Such shifts in the visible spectral region of LaCl_3 : Pr were observed in high-resolution spectra by Dorman.¹³

B. ${}^3F_3 \rightarrow {}^3H_4$ Lifetime Measurements

The shape of the decay of the ${}^3F_3 \rightarrow {}^3H_4$ transition was measured for most of the samples used in plotting Fig. 4. The ${}^3F_4 \text{Pr}^{3+}$ level was pumped until a steady-state population existed in the 3F_3 level. This was achieved by allowing the pump light to remain on for more than ten times the decay lifetime of the longest-lived component of the 3F_3 decay. The decay of the ${}^3F_3 \rightarrow {}^3H_4$ transition could be followed for about five lifetimes before being lost in noise. The pump-light cutoff time was determined by the rate at which the chopper blade crossed the slit and was $\leq 30 \mu\text{sec}$ for all of the experiments. (The cutoff time was the time it took the pump-light intensity to fall from 90% to $< 1\%$ of its former intensity.)

1. Direct Donor-Acceptor Transfer

The decays of the 0.025-at. % Pr (0.0-, 0.1-, and 0.5-at. % Nd) samples are shown in Fig. 5. The solid lines are plots of $\phi_s(t)$ for the dipole-dipole interaction [see Eq. (2)]. Since there is some departure from the nominal concentrations in the samples studied the value for N_a was allowed to vary around its nominal value (by about 20%) to obtain the best fit to the curves. The fits obtained from the dipole-dipole interactions are quite good. Unfortunately $\phi_s(t)$ is not a very sensitive function of the interaction involved. By shifting the concentration from its nominal value (by $\sim 25\%$) reasonable fits to the dipole-quadrupole and quadrupole-quadrupole interactions can be obtained. These fits are not quite as good as the dipole-dipole fit but are close enough so that it is not possible to say unambiguously that dipole-dipole interactions are responsible for the transfer.

2. Effects of Diffusion

The decays for the 0.025-at. % Pr and the 0.25-at. % Pr samples can be fitted using the dipole-dipole interaction and assuming the same value for C for all samples. It is not possible to fit the shape of the decays of the 2-, 5-, or 20-at. % Pr samples (Figs. 6-8) to Eq. (2) (transfer in the absence of diffusion) even if C is varied. The decays of the LaCl_3 : 2-at. % Pr (0.0-, 0.01-, 0.03-, 0.05-, 0.5-, and 1-at. % Nd) samples are shown in Fig. 6. The LaCl_3 : 5-at. % Pr (0-, 0.01-, and 0.05-at. % Nd) and LaCl_3 : 20-at. % Pr (0-, 0.05-, and 0.1-at. % Nd) samples are shown in Figs. 7 and 8. In Fig. 7 an attempt was made to fit the LaCl_3 : 5-at. % Pr, 0.05-at. % Nd decay to the dipole-dipole interaction. The fit is quite poor (the other multipolar interactions give even poorer fits).

In systems in which donor-donor transfer is occurring, $\phi(t)$ (for large values of t) is exponential, with a decay lifetime given by Eq. (5). $\phi_s(t)$, at

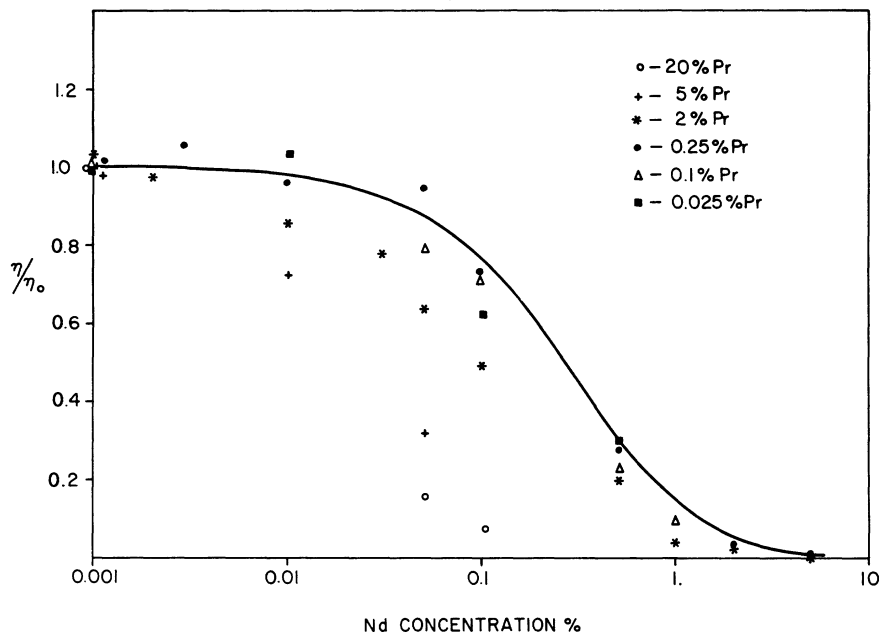


FIG. 4. η/η_0 for the ${}^3F_3 \rightarrow {}^3H_4$ transition (all samples studied). All percentages are atomic.

these values of t , will also be exponential with the same time constant. The value of D , the diffusion constant, is a measure of the donor-donor transfer rate. Measurements of D are easiest to obtain for those decays which show predominantly exponential behavior.

The decays for the 5- and 20-at. % Pr samples are determined by rapid donor-donor transfer and are very nearly exponential. If Eq. (7) is examined for the case of low acceptor concentration and large diffusion constant D , it ap-

proaches an exponential after a short time. The effects of exciton migration can be seen clearly in Fig. 9. Shown there are decay curves for LaCl_3 samples, all of which have 0.05-at. % Nd^{3+} dopant but whose Pr^{3+} content varies from 0.25 to 20 at. %. Values or limits were obtained for D from Eq. (5) for all of the decay curves measured. These diffusion parameters are given in Table I. They were calculated assuming a nominal value for C of 6×10^{-38} cm⁶/sec. C may not remain completely constant due to slight shifts

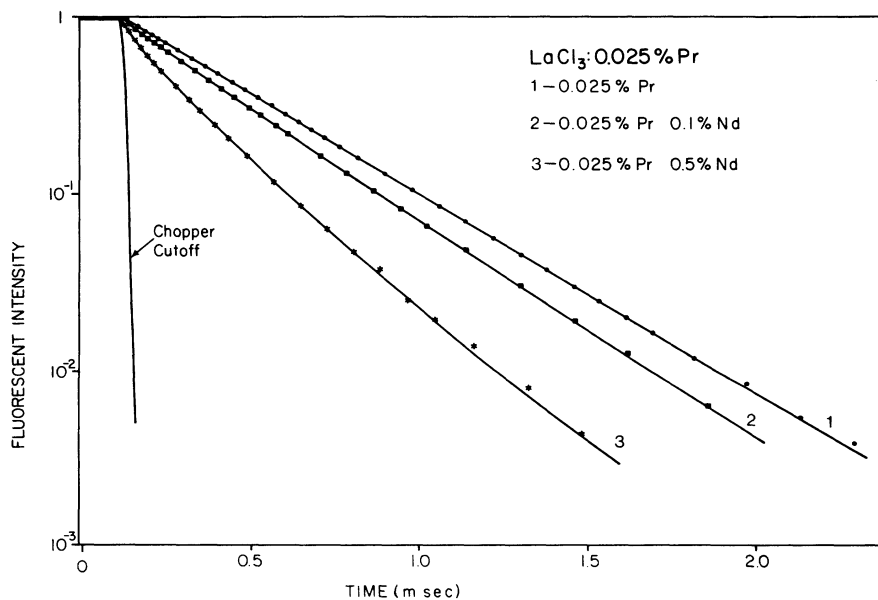


FIG. 5. Decay curves LaCl_3 : 0.025-at. % Pr (0-, 0.1-, and 0.5-at. % Nd). All percentages are atomic.

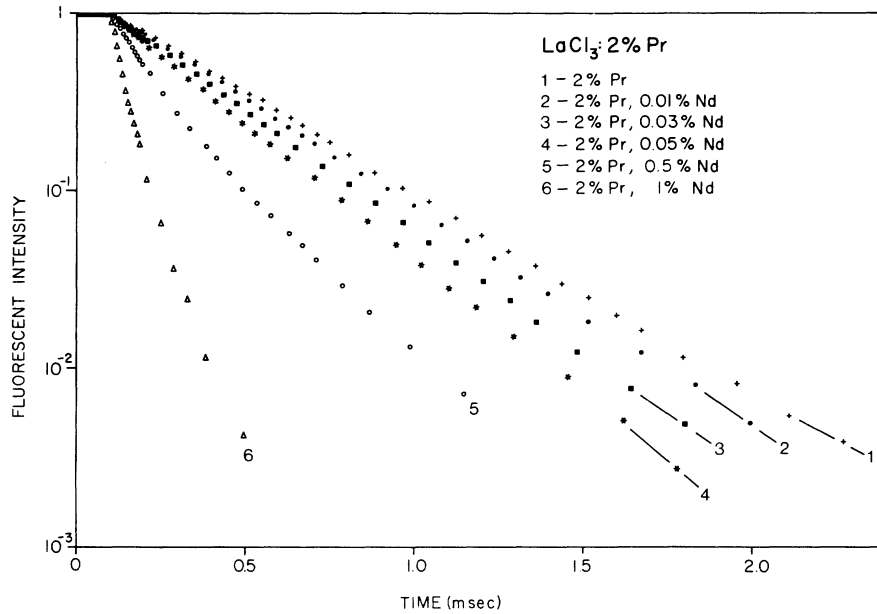


FIG. 6. Decay curves LaCl_3 :2-at.% Pr (0-, 0.01-, 0.03-, 0.05-, 0.5-, and 1-at.% Nd). All percentages are atomic.

in energy-level positions. However, the exponential portion of the decay curves is dependent on $C^{1/4}$ and so even fairly wide variations in C should not alter the parameters appreciably. Also the exponential shape of the decay curves for high Pr^{3+} concentrations is indicative of a diffusion process.

3. Parameters Governing Diffusion

The distance traveled by an exciton in a time t is given by the diffusion length $(Dt)^{1/2}$. If a random walk is assumed for the excitons and we as-

sume a donor-donor transfer distance of 4.8 \AA for the 20-at.% Pr samples, 7.5 \AA for the 5-at.% Pr samples, and 10 \AA for the 2-at.% Pr samples, an estimate of the average donor-donor transfer time can be obtained along with the donor-donor interaction constant. The most probable displacement for a random walk of N steps in three dimensions with step length l is

$$r = l(8N/3\pi)^{1/2}. \tag{8}$$

(The above formula is strictly true only for fixed l and large N .) Setting $r = (Dt)^{1/2}$ and using the

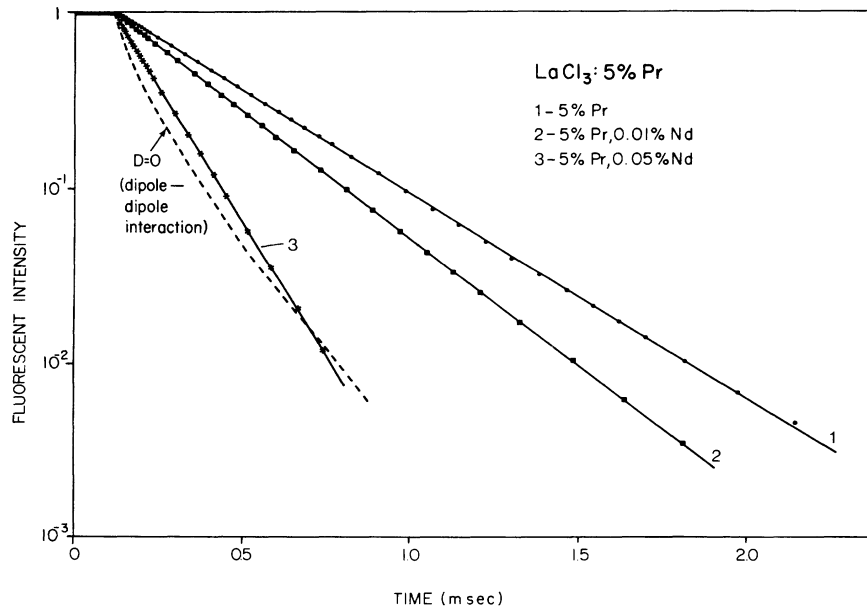


FIG. 7. Decay curves LaCl_3 :5-at.% Pr (0-, 0.01-, and 0.05-at.% Nd). All percentages are atomic.

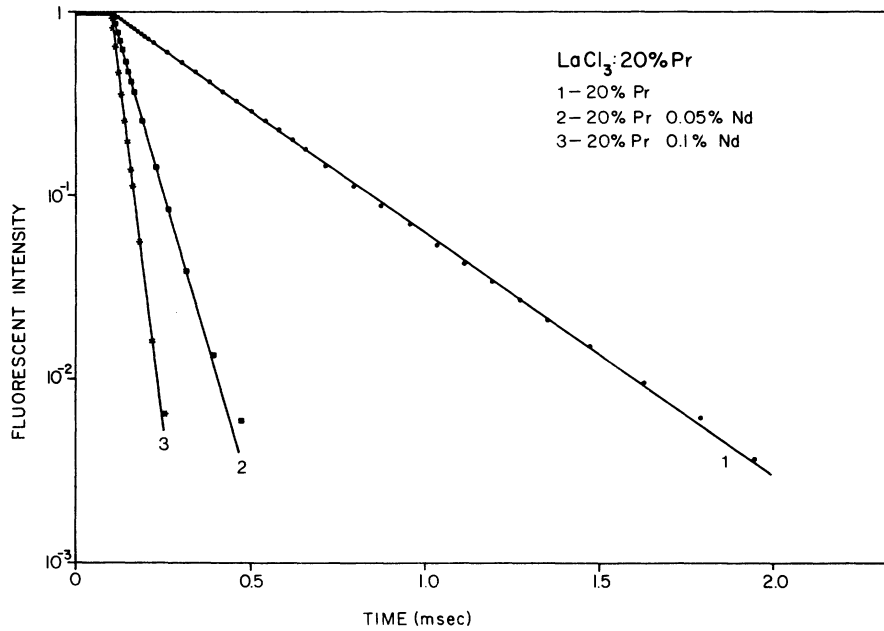


FIG. 8. Decay curves LaCl_3 :20-at.% Pr (0-, 0.05-, and 0.1-at.% Nd). All percentages are atomic.

average donor-donor distance as l will give the average number of steps to travel the distance r . The average time per transfer can then be found by taking the average exciton lifetime and dividing by the number of transfers. As expected, this is independent of the lifetime of the exciton and depends only on the diffusion constant and the step length,

$$T_0 = \frac{8}{3\pi} \frac{l^2}{D}, \quad (9)$$

using the diffusion constants from Table I. The average donor-donor transfer time for the 2% samples is found to be $70 \mu\text{sec}$; for the 5% samples it is $\sim 4 \mu\text{sec}$, and for the 20% samples, $\sim 0.4 \mu\text{sec}$.

If the dipole-dipole interaction is assumed to be responsible for the transfer then a donor-donor interaction constant can be obtained from Eq. (9):

$$C_{dd} = \frac{3}{8} \pi DR^4. \quad (10)$$

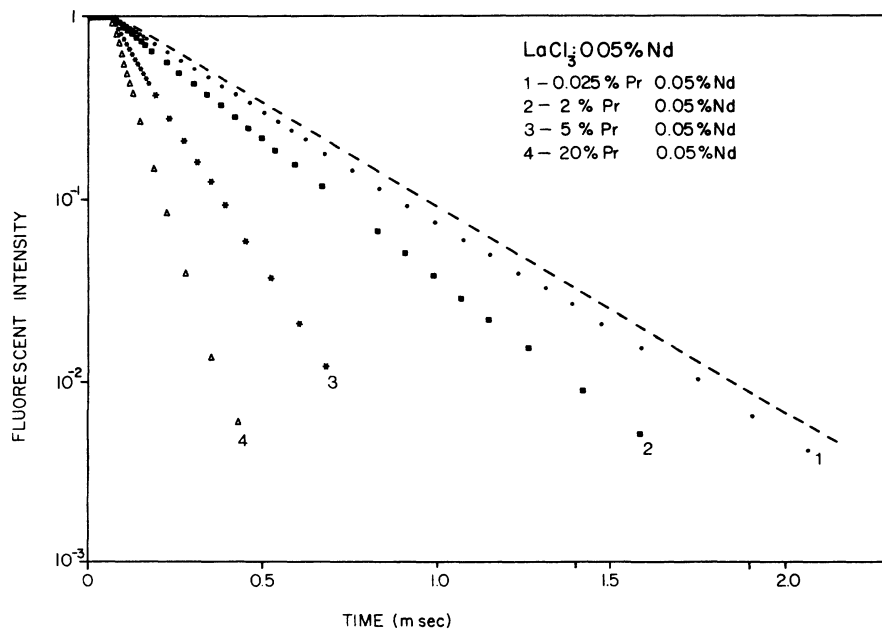


FIG. 9. Decay curves LaCl_3 :0.05-at.% Nd (0.25-, 2-, 5-, and 20-at.% Pr). All percentages are atomic.

TABLE I. Diffusion constant cm^2/sec .

Pr (at. %)	Nd (at. %)					
	0.01	0.03	0.05	0.1	0.5	1
0.025 and 0.25	$< 10^{-11}$					
2	1.3×10^{-10}	1.0×10^{-10}	1.2×10^{-10}	4.8×10^{-11}	$< 1.5 \times 10^{-11}$	$< 8 \times 10^{-11}$
5	1.1×10^{-9}		1.4×10^{-9}			
20			5.0×10^{-9}	6×10^{-9}		

The C_{dd} values are $\sim 1.4 \times 10^{-38} \text{ cm}^6 \text{ sec}^{-1}$ for the 2% samples, $\sim 4.1 \times 10^{-38} \text{ cm}^6 \text{ sec}^{-1}$ for the 5% samples, and $\sim 3.4 \times 10^{-38} \text{ cm}^6 \text{ sec}^{-1}$ for the 20% samples.

If a value of $C = 2 \times 10^{-38} \text{ cm}^6 \text{ sec}^{-1}$ is assumed the effects of donor-donor transfer in the 0.25% samples can be estimated. For Pr concentration of 0.25 at. % this gives $D = 7 \times 10^{-12} \text{ cm}^2 \text{ sec}^{-1}$. The effects of this small amount of diffusion are smaller than the experimental errors in the lifetime measurements.

4. Impurity Content

Knowing the diffusion constant it is possible to estimate the number of impurity ions in the samples. These samples were all grown using La_2O_3 which was certified by the manufacturer to be 99.9999% pure with respect to other rare earths. The Pr_2O_3 and Nd_2O_3 starting materials were 99.999% pure. Other non-rare-earth ions, such as iron, also may be present to act as sinks in the sample. If the transfer rate to the impurity ions in the sample is assumed to be equal to the Pr-Nd transfer rate the reduction in 3F_3 lifetime for the 5% sample is due to an apparent ~ 0.0007 -at. % Nd concentration. For the 20% sample this concentration is ~ 0.0006 %.

5. Fast Diffusion

As the Pr concentration is increased donor-donor transfer becomes very rapid. At high donor concentrations it is possible that exciton diffusion is no longer the rate-limiting step. Instead, the transfer may be determined by the near-neighbor Pr-Nd transfer time or, if a large percentage of the Nd ions are excited, by the lifetime of the excited Nd state. In the latter case both the ratio of the intensities of the ${}^3F_3 \rightarrow {}^3H_4$ and ${}^4I_{15/2} \rightarrow {}^4I_{9/2}$ fluorescences and the 3F_3 decay lifetimes would depend on pump-light intensity; neither of these effects were seen experimentally.

If, for high donor concentration, the rate-limiting step is the donor-acceptor transfer rate rather than the diffusion rate then the diffusion constant would appear to level off with increasing donor concentration. The most rapid decay possible is that for a donor with an acceptor as its nearest neighbor. The possibility of having more than one

acceptor nearby is extremely unlikely for the concentrations of acceptors which have been studied. The nearest-neighbor rate can be obtained from $P = C/R^6$, with $C = 6 \times 10^{-38} \text{ cm}^6/\text{sec}$ and $R = 4.3 \text{ \AA}$; this yields $P = 10^7 \text{ sec}^{-1}$. The only transfer time which is comparable with this rate is that for donor-donor transfer in the 20-at. % Pr samples but in this case the exciton must travel over long distances, $\sim 30 \text{ \AA}$, to reach a Nd ion. The total time which it takes to reach the acceptor will still be much longer than the near-neighbor $\text{Pr}^{3+}\text{-Nd}^{3+}$ transfer rate. There is also a large change in the diffusion constant in going from samples which contain 5-at. % Pr to those which contain 20-at. % Pr showing that, at least for the 5-at. % Pr samples, the donor-acceptor transfer rate is not the decay limitation. An energy-transfer system which appears to be limited by the donor-acceptor transfer rate has been investigated by Watts and Richter.³ They have studied the decay of excited Yb^{3+} donors in the presence of Ho^{3+} acceptors in YF_3 . This is a nonresonant transfer and they find a very small value of C of $1.8 \times 10^{-41} \text{ cm}^6 \text{ sec}^{-1}$ for the transfer so that the near-neighbor transfer rate is only $\sim 10^4 \text{ sec}^{-1}$. In their experiment only a small change in D is observed when the Yb concentration changes from 3% to 10%.

C. $\text{Pr}^{3+} {}^3H_6$ Donor System: Intensity Measurements

The same samples used in studying the ${}^3F_3 \rightarrow {}^3H_4$ system were used for the ${}^3H_6 \rightarrow {}^3F_2$ transition. Since the 3F_2 level relaxes rapidly to the 3H_6 level via phonon emission, no fluorescence was observed from this level. The ${}^3H_6 \rightarrow {}^3H_4$ Pr^{3+} transition and the ${}^4I_{13/2} \rightarrow {}^4I_{9/2}$ Nd^{3+} transition were the only other fluorescences within the experimental range of observation.

The major information concerning the strength of the transfer interaction has been obtained by observing the intensity of the ${}^3H_6 \rightarrow {}^3H_4$ transition with changes in Pr and Nd concentrations. The results of these measurements are shown in Fig. 10. The solid line in Fig. 10 corresponds to a critical-transfer radius of $R_0 = 27 \text{ \AA}$. Since the 3H_6 lifetime via radiative and multiphonon processes is $\sim 20 \text{ msec}^{10}$ while the lifetime for the 3F_3 level is 384 \mu sec , the longer range for the 3H_6 transfer mechanisms is simply a result of having

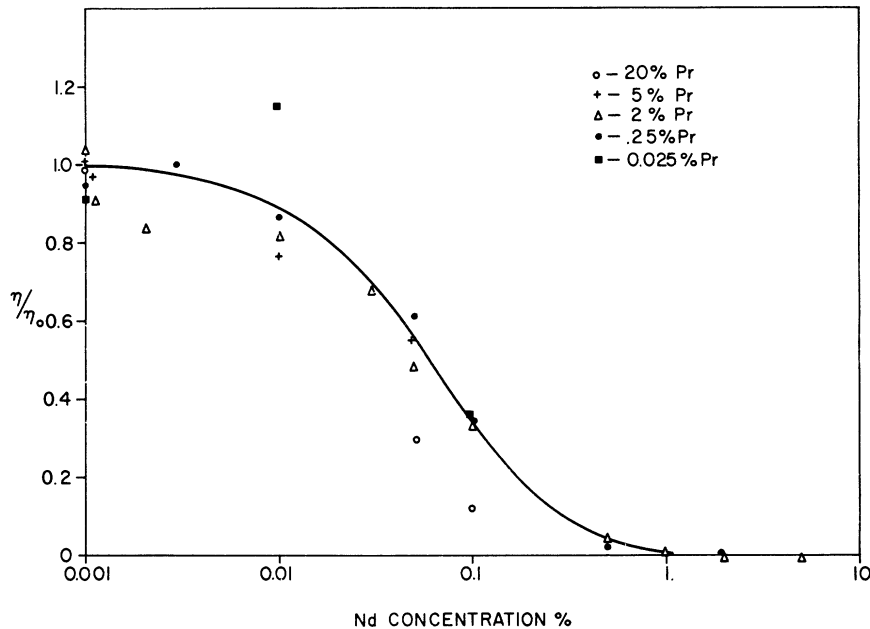


FIG. 10. η/η_0 for the ${}^3H_6 \rightarrow {}^3H_4$ transition. All percentages are atomic.

a longer time in which to interact. The value of C , the energy-transfer interaction strength, is given by R_0^6/τ_0 and is 2×10^{-38} cm⁶/sec, which is smaller than, but still quite similar to, the value of 6×10^{-38} cm⁶/sec found for the 3F_3 donor system.

The curves in Fig. 10 all follow the same basic shape except for the 20-at.-%-Pr curve. This curve falls off much more sharply with increasing Nd concentration. A similar dropoff of η/η_0 for the ${}^3F_3 \rightarrow {}^3H_4$ transition began at 2-at.-% Pr and was the result of donor-donor transfer. The fact that no donor-donor transfer is noticeable in those samples which contain < 20-at.-% Pr seems to indicate a much slower diffusion rate among donors for the ${}^3H_6 \rightarrow {}^3H_4$ transition. It is also possible that the slight energy-level shifts which occur with increasing Pr concentration are changing C and thus masking the effects of diffusion.

The intensity curves for the ${}^3H_6 \rightarrow {}^3H_4$ transition show somewhat more scatter than did the ${}^3F_3 \rightarrow {}^3H_4$ intensity curves. This is not the result of increased experimental measuring errors but rather it occurs because the fluorescence intensity in the latter case is more sensitive to Pr³⁺ content and hence variations in the Pr concentration in each family of a given nominal Pr content lead to a larger scatter.

VI. SUMMARY AND CONCLUSIONS

The energy-transfer mechanisms acting between the low-lying energy levels of Pr and Nd in LaCl₃ have been investigated. The Pr³⁺ 3F_3 and 3H_6 energy levels have several resonant matches for

transfer to the Nd³⁺ ions. At low temperatures these transfers are irreversible, so the effects of these transfers can be seen in a decrease in the fluorescent intensity and lifetime of the donor excited state, and also in an increase in the excited-state population of those ions to which the energy is transferred. The effects of both direct energy transfer and energy migration were studied.

For the samples with low (< 2-at.-%) Pr concentration the experimental results indicated that direct Pr³⁺ to Nd³⁺ transfer was the dominant means of energy transfer. The experimental results were shown to be consistent with a dipole-dipole transfer mechanism. From the intensity measurements donor-acceptor energy-transfer constants were obtained. The values are $C = 6 \times 10^{-38}$ cm⁶ sec⁻¹ for the Pr³⁺- 3F_3 -donor-Nd³⁺-acceptor transfer and $C = 2 \times 10^{-38}$ cm⁶ sec⁻¹ for the Pr³⁺- 3H_6 -donor-Nd³⁺-acceptor transfer. Measurements of the ${}^3F_3 \rightarrow {}^3H_4$ fluorescences are in agreement with the results of the intensity measurements. The decays are nonexponential and can be fit by a dipole-dipole interaction between the Pr³⁺ and Nd³⁺ ions using the same value for C as was obtained from the intensity measurements.

At Pr concentrations \geq 2-at.-% energy transfer between Pr³⁺ ions must be accounted for. At these concentrations the Pr³⁺ ions are near enough to each other to resonantly transfer energy; the excitation can then migrate to the vicinity of a Nd ion, where it will be quenched. A dipole-dipole interaction was assumed for the donor-donor transfer and the exponential portions of the decay curves were used to determine the amount of diffusion

present. The values of the diffusion constants (Table I) are consistent with a donor-donor interaction constant of $C \sim 3 \times 10^{-38} \text{ cm}^6 \text{ sec}^{-1}$. Much of the scatter in the values of the diffusion constant at fixed Pr concentration is attributable to uncertainties in determining the dopant concentrations; however, the reduction in the diffusion constant for the 2-at. % Pr samples as the Nd concentration is raised appears to be systematic. The largest diffusion constants obtained were for the $\text{LaCl}_3\text{:20-at. \% Pr}$ (0.05- and 0.1-at. % Nd) samples, where $D \sim 5 \times 10^{-9} \text{ cm}^2 \text{ sec}^{-1}$. This diffusion constant is much larger than that obtained by Weber¹ of $6 \times 10^{-10} \text{ cm}^2 \text{ sec}^{-1}$ for 100% $\text{Eu}(\text{PO}_3)_3$ glass. This is not surprising since inhomogeneities in the field seen by the ions at different sites in a glass will shift the donor-ion energy-level positions and this may slow the diffusion considerably.

The diffusion constants for the 20-at. % Pr samples are comparable with that of $2 \times 10^{-9} \text{ cm}^2 \text{ sec}^{-1}$ found by Van der Ziel *et al.* in 10% Er:YF_3 .² Concentration quenching studies of the rare-earth-doped trichlorides have been performed by Gandrud and Moos.¹¹ They find, by a different method, slightly faster diffusion.

If donor-donor transfer is very rapid the exciton can move quickly through the lattice and the exciton diffusion time is no longer the rate-limiting step. In such cases the energy transfer may be limited by the transfer rate between the donor ions and near-neighbor acceptor ions. In the present study the energy transfers investigated have been resonant transfer and exciton migration time was much longer than the near-neighbor transfer rate for all samples studied. Hence, the limit of fast diffusion was not reached.

[†]Supported by the U.S. Army Research Office, Durham, N. C.

*Visiting Fellow 1972-1973, Joint Institute for Laboratory Astrophysics-Laboratory for Atmospheric and Space Physics, University of Colorado, Boulder, Colo. 80302.

¹M. J. Weber, *Phys. Rev. B* **4**, 2932 (1971).

²J. P. Van der Ziel, L. Kopf, and L. G. Van Uitert, *Phys. Rev. B* **6**, 615 (1972).

³R. K. Watts and H. J. Richter, *Phys. Rev. B* **6**, 1584 (1972).

⁴For further details, see N. Krasutsky, Ph.D. dissertation (The Johns Hopkins University, 1972) (unpublished).

⁵T. Förster, *Ann. Phys. (Leipz.)* **2**, 55 (1948).

⁶D. L. Dexter, *J. Chem. Phys.* **21**, 836 (1953).

⁷M. Inokuti and F. Hirayama, *J. Chem. Phys.* **43**, 1978 (1965).

⁸P. G. de Gennes, *J. Phys. Chem. Solids* **7**, 345 (1958).

⁹M. Yokota and I. Tamimoto, *J. Phys. Soc. Jap.* **22**, 779 (1967).

¹⁰G. H. Dieke, *Spectra and Energy Levels of Rare Earth Ions in Crystals*, edited by H. M. Crosswhite and Hannah Crosswhite (Interscience, New York, 1968).

¹¹W. B. Gandrud and H. W. Moos, *J. Chem. Phys.* **49**, 2170 (1968).

¹²L. A. Riseberg, W. B. Gandrud, and H. W. Moos, *Phys. Rev.* **159**, 262 (1967).

¹³E. Dorman, *J. Chem. Phys.* **44**, 2910 (1966).

Mössbauer Study of Relaxation Phenomena in $(\text{NH}_4)_3\text{FeF}_6$

S. Mørup and N. Thrane

Laboratory of Applied Physics II, Technical University of Denmark, DK 2800 Lyngby, Denmark

(Received 18 July 1972)

The shape of a relaxation-broadened Mössbauer absorption line for a paramagnetic ferric compound is influenced by various terms of the ionic Hamiltonian. Here we discuss especially how the application of an external magnetic field may influence the line shape and may give information about the magnitudes of other terms of the ionic Hamiltonian. Measurements on the two phases of $(\text{NH}_4)_3\text{FeF}_6$ demonstrate differences between cubic and noncubic surroundings of the ferric ion. In the cubic phase we have found a temperature-independent spin-correlation time $\tau \approx 1.19 \times 10^{-10} \text{ sec}$.

I. INTRODUCTION

Mössbauer absorption lines of paramagnetic ferric compounds are often broadened due to electronic relaxation. In some cases a narrowing of the lines has been found when a magnetic field is applied.¹⁻⁶ In the cubic compound ferric alum,⁵ $\text{NH}_4\text{Fe}(\text{SO}_4)_2 \cdot 12\text{H}_2\text{O}$, a field of the order of 1 kG reduces the linewidth by about 50%, whereas in the noncubic compound $\text{Fe}(\text{NO}_3)_3 \cdot 9\text{H}_2\text{O}$ ² larger fields

are required to produce an effect. Furthermore, in this case the narrowing is less pronounced. In $\text{FeCl}_3 \cdot 6\text{H}_2\text{O}$ ^{3,4} an asymmetric quadrupole splitting becomes symmetric in a field of about 10 kG. In larger fields the opposite asymmetry is found.⁴ It seems that the influence of the applied field on the spectra depends both on the crystal-field parameters, the magnetic interaction of the ions, and the magnitude of the quadrupole interaction.

In order to further study these phenomena we